NUMERICALLY DETERMINED PRESSURE FIELDS APPLIED TO HEAT TRANSFER SIMULATION IN THE SARA TPS

Humberto Araujo Machado, humbertoam@iae.cta.br
Algacyr Morgenstern Júnior, algacyr@iae.cta.br
Instituto de Aeronáutica e Espaço- IAE, Pç. Mal. Eduardo Gomes, 50, Vila das Acácias, São José dos Campos, SP, 12228-904

Abstract. *In this work, numerical simulations of the flow field for different instants of the SARA Sub-orbital platform trajectory are performed to be used in the determination the flow thermal properties. These results are employed in the solution of the coupled conduction-ablation problem in the TPS (thermal protection system) of SARA. The Interface Tracking Method is used to solve the moving boundary problem. The pressure field in the vehicle surface, obtained from the numerical simulation, is used to estimate the film coefficient and compared to that obtained from the usual approximation, the Newton's Pressure Method. Results for the region near the stagnation point of SARA show that, although significant differences in the coefficients appear, the temperature field and ablation rate are quite close for both methods of surface pressure estimation, allowing the use of the models and computational tools developed in this work for studying and dimensioning of thermal protection for hypersonic flight.*

Keywords*: Numerical simulation, High speed flows, Aerodynamic heating, Ablation.*

1. INTRODUCTION

Space and sub orbital vehicles reach high speeds within the atmosphere, i.e., below 100 km of altitude. Such high velocities result in aerodynamic heating. The heat exchange at the wall surface involves heat convection and thermal radiation processes. In the case of recoverable payloads, the heating occurs in both, ascendant and reentry trajectories. Air temperature surpasses 2000^{o} C at the stagnation point (Machado & Pessoa Filho, 2007). As a consequence, aerodynamic heating plays a very important role in the vehicle design. Besides the effects of high temperatures on the mechanical behavior of the structure and onboard devices, it is mandatory to preserve the payload, by using an efficient TPS (*Thermal Protection System*). TPS design is a critical aspect of a rocket design, since its under dimensioning may result in the loss of the payload and the over dimensioning implies in increasing weight and cost. For many years ablative materials have been effectively used as TPS of space vehicles. Ablation involves phase change and chemical reactions. In these processes the kinetic energy of the rocket is converted into heat, which consumes the TPS through ablation (Rogan & Hurwicz, 1973). It is a complex phenomenon, related with several physical processes happening simultaneously (Silva, 2001).

The coupling between the heat transfer processes in the surface and within the layers represents an additional difficulty. The external heat exchange occurs by convection and radiation, and the heat transfer to the wall (TPS and structure) occurs by conduction. In order to obtain the temperature profile and the heat load in the structure, the energy conservation equation has to be solved. A common approach is to consider the heat conduction as one-dimensional, in the normal direction relative to the local surface. However, such hypothesis becomes inaccurate as temperature gradients in the tangential direction, change of material or a great thickness variation occur (Mazzoni et al, 2005).

The convective heat transfer coefficient can be estimated through some engineering methods, based on empirical results. Usually, the models employed are based extensively in Eckert's reference enthalpy (Hurwicz and Rogan, 1973) where the heat transfer inside a compressible boundary layer can be estimated through the relations for incompressible flow, with all properties evaluated in the reference condition. This calculation is strongly dependent on the surface pressure where the heat exchange occurs.

The pressure within the boundary layer can be calculated through the solution of the complete boundary layer equations, via computational simulation and employing a discrete method, for example. However, such way of solution demands a high computational effort that is not desirable during the initial phases of vehicle design. In this case, some approximate methods are used, in order to get results that are accurate enough for the design development. Usually the Newton's Method (Anderson, 1989) is employed, which basically involves geometry description concerned to the flow filed around the surface. This method presents good accuracy when applied near the stagnation point, in velocities higher than Mach five. Although the strongest heating occurs in these conditions, it is necessary to estimate the heat transfer in other regions and velocities as well.

The objective of this work is to present a computational simulation of the aerodynamic heating and ablative process in the vicinity of the stagnation point during the flight of the SARA Sub-orbital Platform, taking into account the effects of the two-dimensional conduction within the TPS. The surface pressure, used for heat transfer coefficient estimation, is determined through the solution of the N-S equations, employing the Spalart&Allmaras (Morgenstern Jr. et al, 2007) turbulence model, and compared with the results of the Newton's method. Such procedure will allow a more accurate dimensioning of the TPS, contributing for project optimization.

The SARA Sub-orbital Platform. Fig.1, is planned as a recoverable platform for experiments in microgravity environment, and is being developed by the Institute of Aeronautics and Space (IAE) of Brazil. It has a total weight of 250 kg and a payload of 25 kg. The orbital version will be able to perform microgravity experiments and keep in an orbit of 300 km during 10 days (Moraes, 1998). SARA trajectory characteristics are showed in Fig. (2)

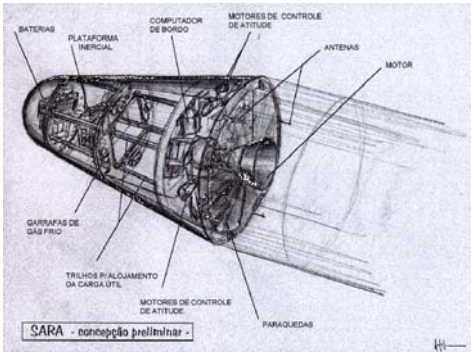

Figure 1. SARA and its subsystems.

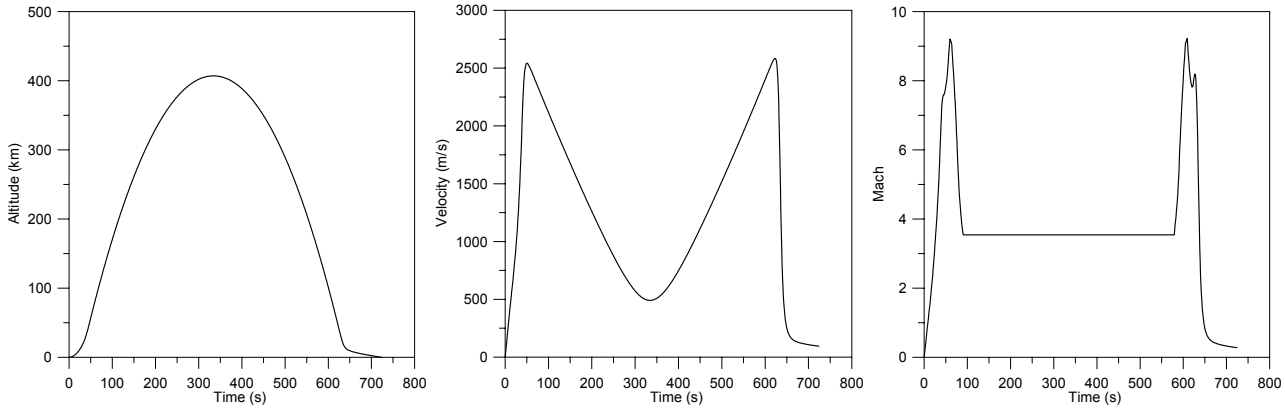

Figure 2. Trajectory of SARA sub-orbital.

2. PHYSICAL PROBLEM AND MATHEMATICAL MODEL

2.1. Aerodynamic heating

To predict the heat transfer on SARA, it is necessary to know pressure, temperature and velocity fields around the vehicle. That can be accomplished by numerically solving the N-S equations. However, such a procedure is expensive and time consuming. In the present work a simpler, but reliable, engineering approach is also used. The following simplifying assumptions are made:

- Zero angle of attack;
- VSB-30 rotation around its longitudinal axis is neglected;
- Atmospheric air is considered to behave as a calorically and thermally perfect gas (no chemical reactions); and

The free stream conditions ahead of the nose cap are those given by v_∞, T_∞, p_∞, corresponding, respectively, to velocity, temperature and pressure. By knowing v_∞ and altitude, as function of time, together with an atmospheric model (U.S. Standard Atmosphere, 1976), it is possible to evaluate the free stream properties, such as p_∞, T_∞, and c_∞, which represent free stream pressure, temperature and speed of sound, respectively. For supersonic flow ($M_\infty > 1$), a detached shock wave appears ahead of the nose. By using the normal shock relationships (Anderson, 1990), it is possible to calculate v_1, T_1 and p_1 after the shock.

The heat flux over the external surface was calculated through the Zoby's method (Zoby et al, 1981; Miranda & Mayall, 2001), namely:

$$q = H\,(T_{aw} - T_w) \tag{1}$$

where q is heat flux, T_w is the wall temperature and T_{aw} is the adiabatic wall temperature, also called recovery temperature, T_r, given by:

$$T_{aw} = T_e + F_R \frac{v_e^2}{2c_p} \tag{2}$$

where c_p is the specific heat, T_e the temperature and v_e the velocity. The subscript e refers to conditions at the boundary layer edge. F_R is the recovery factor, equal to $\sqrt{Pr_w}$, for laminar flow and $\sqrt[3]{Pr_w}$ for turbulent flow. Pr_w is the Prandtl number evaluated at wall temperature, $Pr_w = 0.71$. The convective heat transfer coefficient comes from the Reynolds analogy, namely:

$$H = 0.5\rho_e c_p v_e \, Pr_w^{-a} \, C_F \tag{3}$$

where a is equal to 0.6 for laminar flow and 0.4 for turbulent flow. To take into account compressibility effects, a modified friction factor is obtained (Anderson, 1989)

$$C_F = K_1 (Re_\theta)^{K_2} \left(\frac{\rho_e^*}{\rho_e} \right) \left(\frac{\mu_e^*}{\mu_e} \right)^{K_3} \tag{4}$$

In the equation above, Re_θ is the Reynolds number, based on the boundary layer thickness, θ:

$$Re_\theta = \frac{\rho_e V_e \theta}{\mu_e} \tag{5}$$

The superscript "*" refers to properties evaluated at Eckert's reference temperature (T_e*). Viscosity, μ, is evaluated according to Sutherland´s equation, as function of temperature (Anderson, 1989) and ρ is the specific mass. In Eq.(4) $K_1 = 0.44$, $K_2 = -1$ and $K_3 = 1$, for laminar flow. For turbulent flow, $K_2 = K_3 = -m$, and

$$K_1 = 2 \left(\frac{1}{C_5} \right)^{\frac{2N}{N+1}} \left[\frac{N}{(N+1)(N+2)} \right]^m \tag{6.a}$$

$$m = \frac{2}{N+1} \tag{6.b}$$

$$C_5 = 2.2433 + 0.93N \tag{6.c}$$

$$N = 12.76 - 6.5 \log_{10}(Re_\theta) + 1.21 [\log_{10}(Re_\theta)]^2 \tag{6.a}$$

For laminar flow, the boundary layer thickness is given by (Anderson, 1989):

$$\theta_L = \frac{0.664 \left(\int_0^y \rho_e^* \mu_e^* v_e R^2 dy' \right)^{\frac{1}{2}}}{\rho_e v_e R} \tag{7}$$

where y is measured along the body's surface and $y=0$ corresponds to the stagnation point, and R is a geometric parameter schematically shown in Fig. 3, were the curved red line represents the nose cap surface.

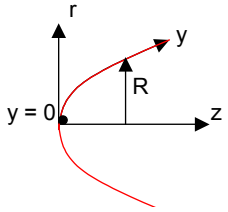

Figure 3. Coordinate system.

In this work the numerical integration of Eq. (7) was obtained according to the trapezoidal method. As $R \rightarrow 0$, Eq. (7) becomes undetermined. By taking the limit of Eq. (7) as $R \rightarrow 0$, the following expression is obtained (Miranda & Mayall, 2001):

$$\theta_L = \frac{0.332\left(\rho_e^* \mu_e^*\right)^{\frac{1}{2}}}{\rho_e \sqrt{\frac{1}{R_N}\left[\frac{2\left(p_s - p_\infty\right)}{\rho_s}\right]^{\frac{1}{2}}}} \tag{8}$$

In this work Eq. (8) is applied for $y < 0.1\ R_N$, where R_N is the radius of curvature at the stagnation point.

The boundary layer thickness for turbulent flow is obtained by solving the following first order differential equation:

$$\frac{D\left(\rho_e v_e R\ \theta_T\right)}{Dy} = 0.5 C_F \rho_e v_e R \tag{9}$$

After obtaining the boundary layer momentum thickness, θ, Re_θ, C_F and H can be evaluated by using Eqs. (5), (4) and (3), respectively. Along the transition region between laminar and turbulent flow, the following relationship is used[11]:

$$q_{Tr} = q_L + F(y)(q_T - q_L) \tag{10}$$

where the subscripts Tr, L and T represent, respectively, transitional, laminar and turbulent flow. The transitional factor, $F(y)$, is given by (Dhavan & Narasinha, 1958):

$$F(y) = 1 - exp\left\{-0.412\left[\frac{4.74\left(y - y_L\right)}{\left(y_T - y_L\right)}\right]\right\} \tag{11}$$

Transition is supposed to occur for $163 < Re_\theta < 275$.

Properties evaluation at the boundary layer edge is performed assuming isentropic flow between the stagnation region and the location "i" where properties are needed, namely

$$\rho_{e,i} = \rho_s \left(\frac{p_{e,i}}{p_s}\right)^{\frac{1}{\gamma}} ; \quad h_{e,i} = h_s \left(\frac{p_{e,i}}{p_s}\right)^{\frac{\gamma-1}{\gamma}} ; \quad v_{e,i} = \sqrt{2\left(h_s - h_{e,i}\right)} ; \quad T_{e,i} = \frac{h_{e,i}}{c_p} \tag{12}$$

The local pressure, $p_{e,i}$, is obtained from the modified Newton´s method (Anderson, 1989; Machado & Villas-Boas, 2006) and $\gamma=1.4$. In this work, this pressure was also obtained by solving the N-S equations (Morgenstern et al, 2007). The results of both methods are then compared. The subscript "s" appearing in Eqs. (12) refers to the stagnation condition. Eckert's reference temperature is obtained from (Anderson, 1989):

$$\frac{T_{e,i}^*}{T_{e,i}} = 1 + 0.032 M_{e,i}^2 + 0.58\left(\frac{T_W}{T_{e,i}} - 1\right) \tag{13}$$

The solution procedure can be summarized as follows:

i. From a given trajectory the US Standard Atmosphere (1976) is used to obtain the free stream properties, including the stagnation ones;
ii. Normal shock relationships are used to obtain the fluid flow properties behind the shock;
iii. By using the modified Newton method, pressure distribution is obtained along the payload;
iv. Equations (12) provide the local properties at the boundary layer edge;
v. If $y < 0.1\ R_N$, Eq. (8) provides the laminar boundary layer thickness, leading to the estimation of Re_θ, C_F and H, provided by Eqs. (5), (4) and (3), respectively;
vi. If $y > 0.1\ R_N$ and $Re_\theta < 163$, Eq. (7) is numerically integrated up to the location where the momentum thickness is to be estimated. Such an integration is performed by using the trapezoidal method;
vii. If $y > 0.1\ R_N$ and $Re_\theta > 275$, Eq. (9) is numerically integrated by the trapezoidal rule leading to the turbulent boundary layer thickness;
viii. If $y > 0.1\ R_N$ and $163 < Re_\theta < 275$, Eqs. (10) and (11) are used to estimate H;

It should be pointed out that such a procedure is performed along the payload's surface (following the y-coordinate), for different trajectory times. Therefore, $H=H(y,t)$.

2.2. Pressure distribution

Pressure distribution over the SARA surface was determined by simulating the flow field with a numerical solution of the governing equations. The Navier-Stokes equations were solved by discretizing the equations with a second order accurate Euler three-point backward time discretization. A finite volume approach is used in the treatment of the spatial discretization of the fluxes with second order central differences. A suitable choice of the factorization procedure yields a scheme with fast convergence and low computational time per iteration (Morgenstern & Moraes, 2003; Morgenstern et.al. 2007). The flow fields considered in these simulations were determined as a function of the SARA predicted trajectory. Hence, the flow conditions considered in these simulations were those presented in Table 1.

Table 1. Flow field trajectory conditions for SARA.

Mach	Reynolds
3,56	18,06 10^6
5,1	6,558 10^6
7,0	1,697 10^6
8,1	3,1 10^4

The results of the numerical simulations over the upper region of SARA for the flow conditions considered are presented in Fig. 4 in the form of isometric lines of constant Mach number in a chromatic scale of Mach number intensity. These plots show the characterization of the flow field with a subsonic region in the vicinity of the stagnation point, the acceleration of the flow as it moves over de spherical region of the ogive up to the conical region of the geometry. The shock stand-off distance and the inclination of the shock wave as a function of Mach number can also be seen.

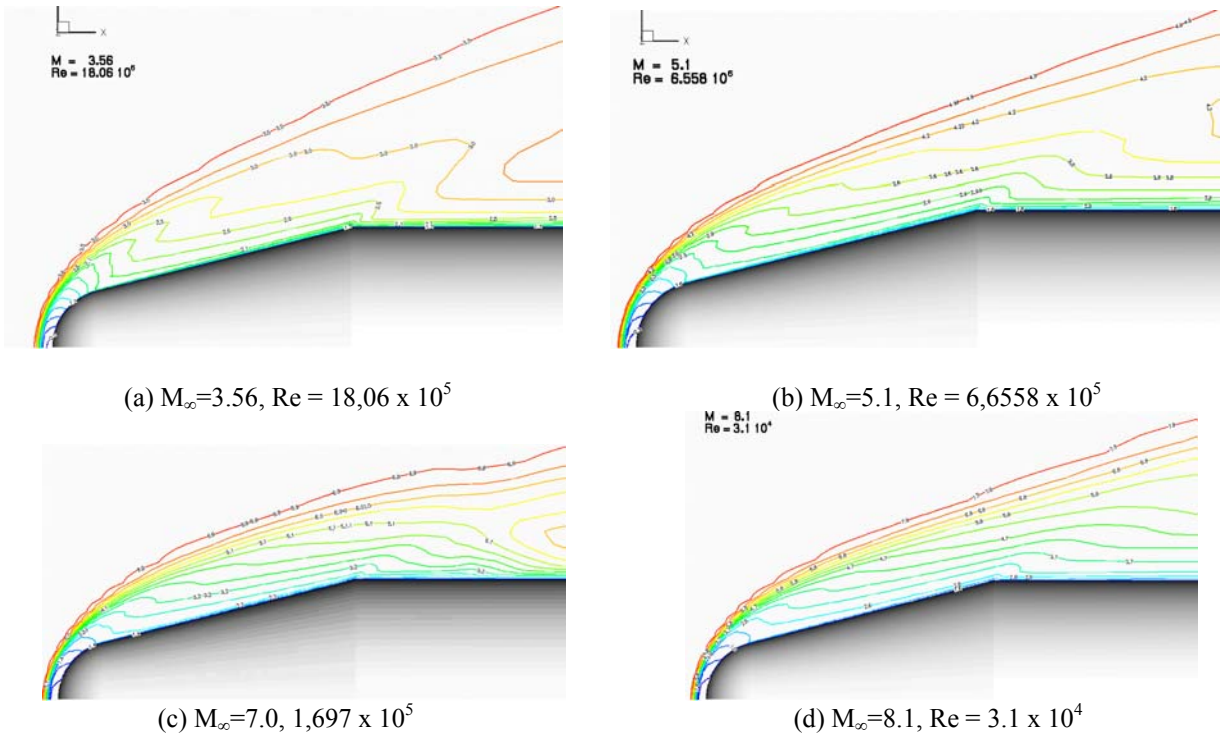

(a) M_∞=3.56, Re = 18,06 x 10^5

(b) M_∞=5.1, Re = 6,6558 x 10^5

(c) M_∞=7.0, 1,697 x 10^5

(d) M_∞=8.1, Re = 3.1 x 10^4

Figure 4. Mach numbers isometric lines of.

The pressure distribution is shown in Fig. 5, starting at the stagnation line of the flow, up to the stagnation point on SARA surface, following along its surface for the flow fields considered. It can be observed the shock stand-off distance as a function of Mach number, characterized by the start of the pressure jump, with the distance from the ogive getting smaller as the Mach number increases. After going through the shock wave, with the deceleration of the flow in the subsonic region, it can be seen a pressure rise up to its maximum value at the stagnation point on the SARA ogive. Following along the spherical region of the nose, a steep reduction in pressure can be observed, with a corresponding increase in velocity, and the flow field returning to a supersonic regime. The following conical region presents an almost constant pressure distribution, with a negative pressure jump due to the pressure expansion on the geometric transition from the conical to cylindrical regions of SARA.

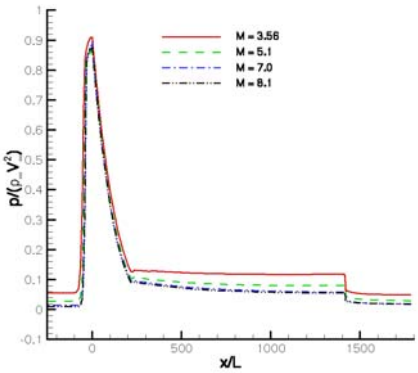

Figure 5. Pressure distribution comparison along the SARA surface.

2.3. Heat conduction and ablation

Once the convection heat transfer and the adiabatic wall temperature are known, wall temperature distributions can be obtained. SARA Sub-orbital platform nose cap is made of a composite material (Si-Phenolic), which works as an ablative TPS. Until the ablation temperature is reached, we have a transient heat conduction problem. Once the TPS surface reaches the ablation temperature, its thickness is reduced; therefore, a transient, coupled conduction moving boundary problem appears. Although ablation in a composite material is a complex phenomenon, involving simultaneously physical and chemical processes, in this work it will be treated as a single-phase change problem, where a representative value for the latent heat of sublimation will be used as the heat of ablation. Such a technique allows for the estimation of the instantaneous position and velocity of the moving boundary corresponding to the surface of the nose cap, from now on called the interface between the solid region and the airflow.

The set of equations used to represent the physical problem is written according to the interface tracking method (Juric, 1996). The nose cap and the airflow around it are represented as parts of a continuous domain of calculation. The application of the energy conservation principle to an infinitesimal volume element of the mathematical domain, Fig. 4, leads to a partial differential equation for the temperature, namely:

$$\frac{\partial(\rho.C_p.T)}{\partial t} = \nabla.K\nabla T + Q \tag{14}$$

where K is the thermal conductivity and Q is a source term that takes into account the net heat exchange at the boundary (Machado & Villas Boas, 2006):

$$Q = \int_A q\,\delta(x - x_F)\,dA \tag{15}$$

where $\boldsymbol{x}$ is the position in the coordinate system, V is the interface velocity, and q is the source term of energy per unit of surface of the interface:

$$q = \rho L V + H(t,y)\left[T_F(t,x_F) - T_{aw}\right] + \varepsilon\sigma\left[T_F^4(t,x_F) - T_\infty^4\right] \tag{16}$$

where L is the heat of ablation.

Although the airflow is included in the domain, its effects are implicit in the convection coefficient H. As a consequence, this region is considered adiabatic, and the heat capacity and thermal conductivity are assumed to be null. Once ablation temperature is reached, the interface condition becomes:

$$T_F - T_A = 0 \tag{17}$$

3. METHOD OF SOLUTION

The moving boundary problem was solved by the Interface Tracking Method, introduced by Unverdi & Trygvason (1992), and employed by Juric (1996) in the solution of phase change problems. In this method, a fixed uniform Eulerian grid is generated, where the conservation laws are applied over the complete domain. The interface acts as a Lagragean referential, where a moving grid is applied. The instantaneous placement of the interface occurs through the constant remeshing of the moving grid, and each region of the domain is characterized by the Indicator Function, which identifies the properties of the wall and the air around it.

This method allows for the representation of any geometry used in the TPS, and also the characterization of every wall layer (structure plus TPS) separately. It is accomplished without a high increase in the computational cost and does not need any pre-processing (construction of unstructured grid or coordinate transformation). In this work, this method is employed to estimate the ablative performance of the TPS, considering a two-dimensional approach in both, the heat conduction and the moving boundary problem.

The interface is represented as a parametric curve, ***R(u)***, where the normal and tangent vectors and curvature are extracted from. The interface points are interpolated by a Lagrange polynomial, which allows one to obtain the geometric parameters and remeshes the curve, keeping the distance *d* between curve points within the interval 0.9 < d/h < 1.1, where *h* is the distance among the fixed grid points, as shown in Fig. 6.

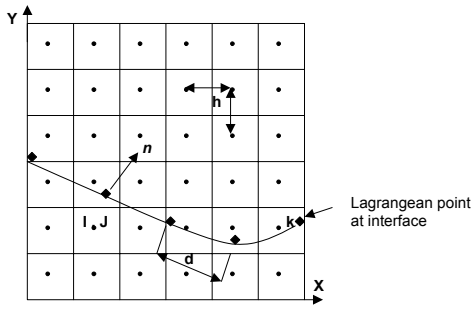

Figure 6. Eulerian and Lagrangean meshes**.**

The Indicator Function varies from 1 (air) to 0 (solid), and it is numerically constructed using the interface curve to determine a source term ***G(x)***. The jump across the interface is distributed over the fixed grid points, yielding a gradient field in the mesh:

$$G(x) = \nabla I = \int_A n\delta(x - x_f)dA \tag{18}$$

which should be zero, except over the interface, as represented by the Dirac delta function, δ. However, such a representation is not convenient for a discrete number of points. The Distribution Function is used to represent the interface jump. Such a function is similar to a Gaussian distribution function and its value depends on the distance $|\boldsymbol{x}_{ij} - \boldsymbol{x}_k|$ between the Lagrangean and Eulerian points:

$$D_{ij}(x_k) = \frac{f[(x_k - x_i)/h].f[(y_k - y_j)/h]}{h^2} \tag{19}$$

where D_{ij} is the Distribution Function for a point *k* in the Lagrangian mesh with respect to a Eulerian point. One should note that increasing *h*, the interface becomes thicker. The function *f* is the probability distribution, Fig. 7, related to the distance *h* as (Unverdi & Tryggvason, 1992; Juric, 1996):

$$f(x) = \begin{cases} f_1(x) & if \ |x| \le 1 \\ 1/2 - f_1(2 - |x|) & if \ 1 < |x| < 2 \\ 0 & if \ |x| \ge 2 \end{cases} \quad ; \quad f_1(x) = \frac{3 - 2.|x| + \sqrt{1 + 4.|x| - 4x^2}}{8} \tag{20.a,b}$$

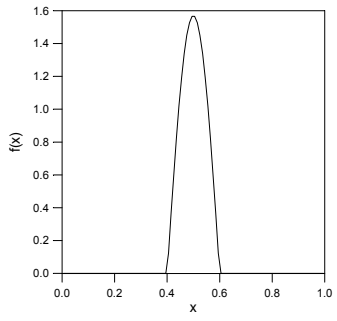

Figure 7. Probabilistic distribution profile.

The divergence of the gradient field is found by numerical derivation of Poison's equation:

$$\nabla^2 I = \nabla . G \tag{21}$$

Despite being considered constants in each phase, the properties inside the domain must be treated as variable in the formulation. A generic property ϕ (ρ, μ, Cp or K) is expressed as:

$$\phi(\xi) = \phi_l + (\phi_v - \phi_l)\, I(\xi,\tau) \tag{22}$$

The coupling between the moving mesh and the fixed grid is done at each time step, through the Distribution Function, that represents the source terms in the balance equations and interpolate the fields with infinitesimal discontinuities into a finite thick region at the interface.

The initial interface shape, $\boldsymbol{R(u)}$, is first specified and then the Indicator Function is constructed. From the initial conditions, the property and temperature fields are determined. Out of the ablative period, the interface temperature keeps bellow the ablation temperature, and the energy equation is solved as a pure heat conduction problem, via the Finite Volume Method, employing an explicit time marching schedule.

As the interface reaches the ablation temperature at a given point, an iterative process starts up, in order to determine the interface velocity at each time step, which must satisfy the temperature condition, Eq.(17), at that interface point. The process goes on as far as the point temperature is equal to ablation temperature. The steps to be followed are:

1. Using the current value of $\boldsymbol{V}$, the interface points are transported to a new position, calculated explicitly through the equation $\boldsymbol{V}^n = (d\boldsymbol{x}_f/dt).\boldsymbol{n}$;
2. Density and specific heat are calculated at the new interface position;
3. $\boldsymbol{V}^{n+1}$ is estimated via Newton iterations, using a numerical relaxation schedule.
4. Heat flux q crossing the interface is calculated through Eq. (16) and distributed into the fixed grid;
5. According to the boundary conditions, energy equation, Eq. (14), is used to obtain the temperature at time step $n+1$;
6. Temperature is interpolated to find T_F at the interface;
7. The jump condition is tested and if it is lower than the reached tolerance, the fields of viscosity and conductivity are updated for the new position, and one step in time is advanced. If that is not the case, a new estimate for $\boldsymbol{V}^{n+1}$ is calculated and the process returns to step 5.

The convergence criterion used in step 7 is the residual in Eq. (17). Once it has reached the desired tolerance, convergence for interface velocity is assumed. Otherwise, the velocity is corrected via Newton Iterations (Unverdi & Tryggvason, 1992; Juric, 1996), given as:

$$V^{n+1} = V^n - \omega . R(T) \tag{23}$$

where ω is a constant and $R(T)$ is the residual for the temperature jump condition at the interface. Iterations are repeated until $R(T)$ in every point become smaller than the prescribed tolerance. The optimum value for ω is found by tentative, at the beginning of the calculation. The method was compared with the analytical solution for a simple phase change problem (Ruperti, 1991), resulting in an excellent agreement.

4. RESULTS

The results were obtained for the region near the stagnation point of SARA Sub-orbital platform, which corresponds to a circular segment with radius 279 mm and base diameter of 1015 mm. Since the flight is considered with zero angle of attack, the problem is axy-symmetric. A 60 x 50 grid over a domain of 6 mm x 5 mm was used, with a tolerance of 10^{-6} in Eq. (18). A resulting 68 points Lagrangean mesh was obtained from the interface. Properties considered for Si-Phenolic composite were (Gregori et al, 2008): $Cp = 1256$ kJ/kg.K, $\rho = 1730$ kg/m^3, $K = 0.485$ W/m.K, $L = 12$ MJ/kg, $T_A = 538^o$ C and $\varepsilon = 0.8$. As initial condition, temperature in the whole domain was taken as $T_0 = 27^o$ C.

4.1. Validation

Initially, the program was employed to estimate the aerodynamic heating and ablation at the stagnation point of SARA and the results were compared with that from 1-D calculation. In Fig. 8.a, the film coefficient and recovery temperature for stagnation point with the time are plotted. In Fig. 8.b, results for wall temperature (structure plus TPS) are compared for the two ways of solution. Results present good agreement, especially during the ablative period. The small discrepancies may be due to the two-dimensional effects. In Fig. 9, the values obtained for the ablation velocity during the ascendant and reentry periods are quite close. Better results for the interface capturing method can be obtained with the used of a more refined mesh. The small difference observed in the ablation velocity has produced a higher discrepancy in the final thickness, Fig. 10, since the effect of an error in this parameter is cumulative.

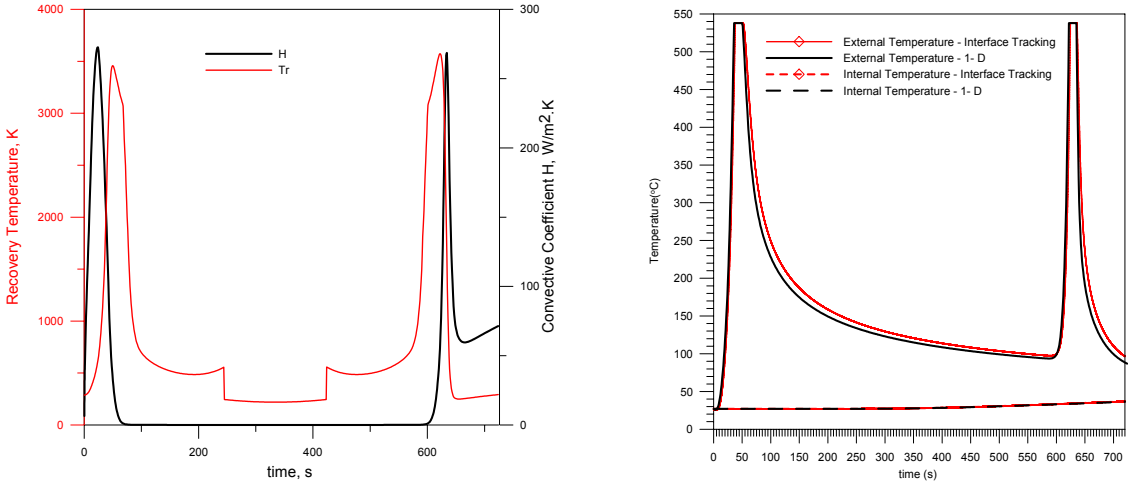

(a) h, Tr **(b) Wall temperatures**

Figure 8. Comparison among 1-D and Interface tracking results at SARA stagnation point.

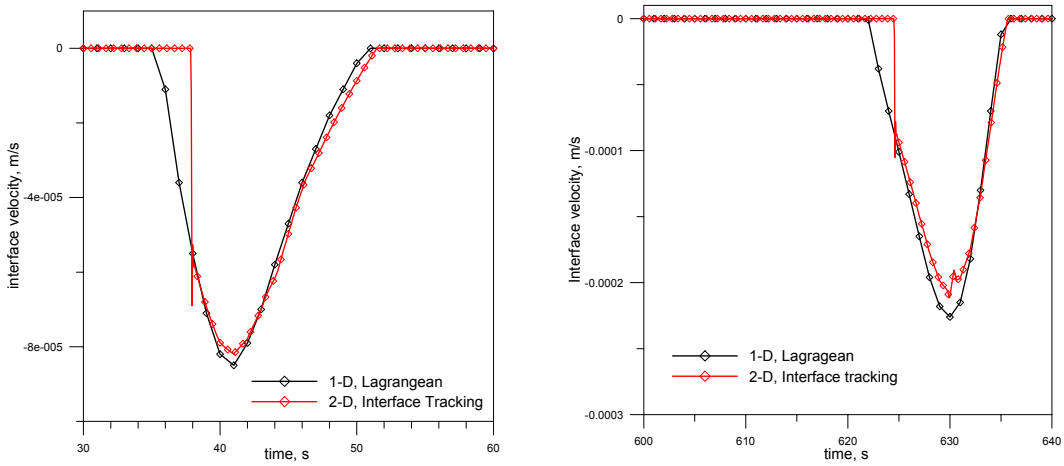

(a) Ascendant period (b) Reentry

Figure 9. Ablation velocity at SARA stagnation point

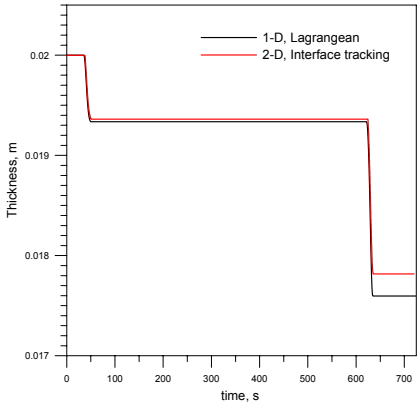

Figure 10. Thickness variation of SARA TPS at stagnation point.

4.2. Two-dimensional solution

Once the program was validated, it was used to simulate the aerodynamic heating during the first 54 seconds of SARA trajectory, employing the surface pressure data obtained from the N-S solution, and compared with results from the use of Newton's Method. Due to some numerical difficulties, in the region very close to the stagnation point, it was used only the Newton 's Method estimative for surface pressure in that region.

In Fig. (11) the Indicator Function and temperature fields are showed, denoting the presence of the interface between the air and the TPS, where the higher variation of these parameters occur. In Fig.(12) results for convective parameters are presented as function of the *y*-coordinate, for several times. As it was mentioned, the values are the same close to the stagnation point and present higher discrepancies far from that region. It is possible to observe a tendency for convergence from a certain point in *y*. However, only the domain extension would verify this behavior.

In Fig. (13.a), the results of the wall temperature for the N-S solution are higher than that from the Newtons's Method. However, as the temperature limit is the ablation temperature, the influence of this parameter in the result of the ablative process is small, as it is showed in Fig. (13.b), where the resulting thickness is the same, as observed by Machado e Villas-Boas (2006).

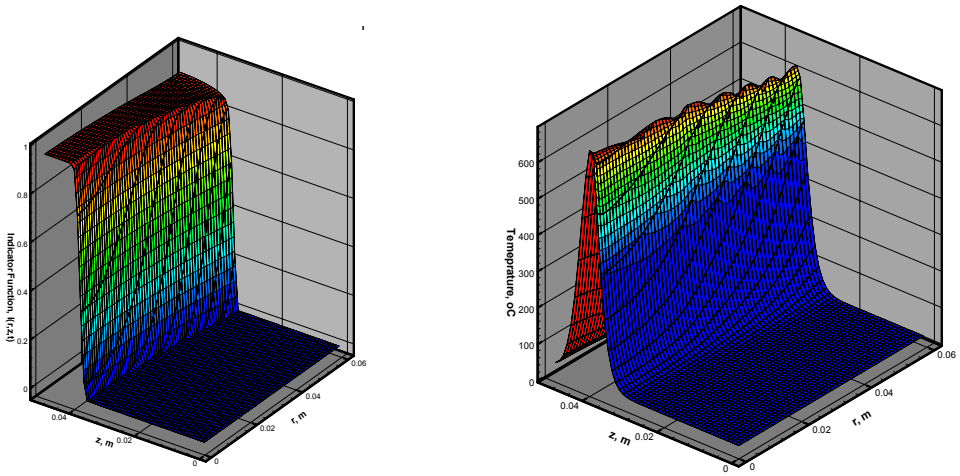

(a) Indicator Function (b) Temperature

Figure 11. Two-dimensional results for t = 54 s.

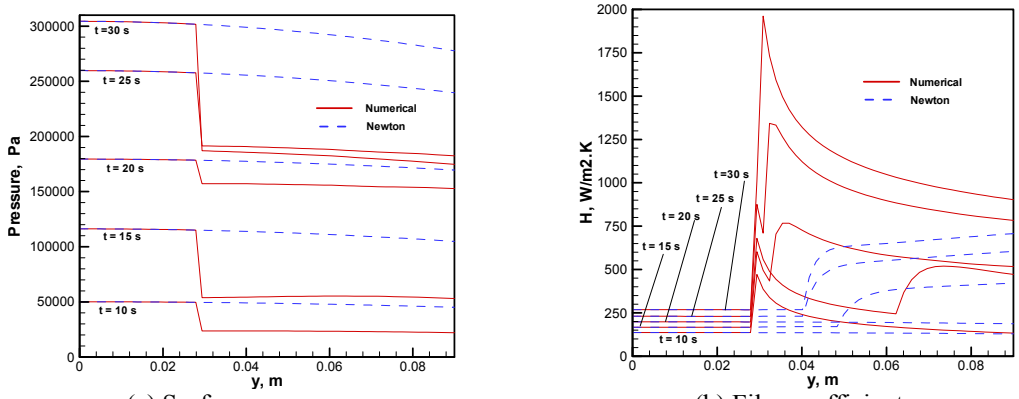

(a) Surface pressure (b) Film coefficient

Figure 12. Convective parameters during the trajectory

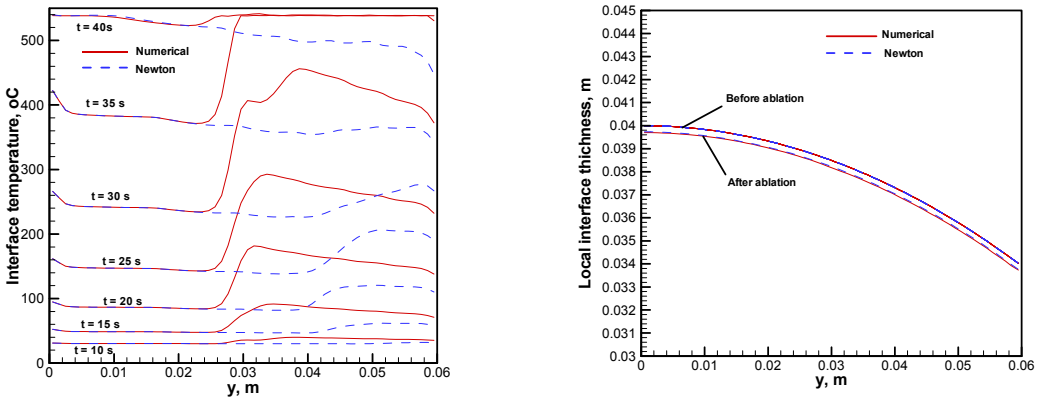

(a) Interface temperature (b) Interface thickness

Figure 13. Ablative parameter during the trajectory.

4. CONCLUSION

In this work, the aerodynamic heating and ablation of the SARA Sub-orbital Platform was simulated. The convection coefficient was estimated using the surface pressure, which was calculated by the N-S solution and by the Newton's Method. The moving boundary problem of TPS ablation was simulated using the Interface Tracking method developed by Unverdi & Tryggvason. After validation of the model with one-dimensional cases, results for two-dimensional solutions employing surface pressures from the Newton's Method and CFD simulations were compared and showed small differences in the final thickness of the TPS, even though the pressure distributions obtained by these two methods presented some discrepancies. As a continuation of this work we intend to extend the solution to the rest of the domain, in order to verify the temperature sensibility to the surface pressure distribution.

3. ACKNOWLEDGEMENTS

The authors would like to thank the Brazilian Space Agency (AEB) for the financial support during this work.

4. REFERENCES

Anderson Jr., J.D., 1990, *Fundamentals of Aerodynamics*, McGraw-Hill, New York.

Anderson Jr., J.D.,1989, *Hypersonic and High Temperature Gas Dynamics*, AIAA Education Series, AIAA, New York,.

Dhawan, S. and Narasimha, R., 1958, "Some Properties of Boundary Layer Flow During the Transition from Laminar to Turbulent Motion," *Journal of Fluid Mechanics*, Vol. 3, No. 4, pp. 418-436.

Gregori, M.L., Barros, E. de A., Petraconi Filho, G., Costa, S.F. and Pardini, L.C., 2008, "Properties of Quartz-Phenolic Composites for Thermal Protection Systems," *59th IAC Congress*, Glascow, Scotland.

Juric, D., 1996, "Computations of Phase Change," PhD. Thesis, University of Michigan.

Machado, H.A. and Pessoa-Filho, J.B., 2007, "Aerodynamic Heating at Hypersonic Speeds," *Proceedings of 19th Brazilian Congress of Mechanical Engineering* [CD-ROM], Brasília, Brazil.

Machado, H.A. and Villas-Boas, D.J.F., 2006, "Comparative Study of Models for Aerodynamic Heating of Space Vehicles," *Proceedings of Brazilian Thermal Sciences Meeting* [CD-ROM], Curitiba, Brazil (in Portuguese).

Mazzoni, J.A., Pessoa Filho, J.B. e Machado, H.A.,2005, "Aerodynamic Heating on VSB-30 Sounding Rocket," *Proceedings of 18th Brazilian Congress of Mechanical Engineering* [CD-ROM], Ouro Preto, Brazil.

Miranda, I.F. and Mayall, M.C de M., 2001, "Convective Heat Flux in Micro-Satellites during the Atmospheric Reentry," Graduate Dissertation, Air Force Technical Institute - ITA, São José dos Campos, Brazil (in Portuguese).

Moraes Jr., P., 1998, "Design Aspects of the Recoverable Orbital Platform SARA", Proceedings of 8th Chilean Congress of Mechanical Engineering, Concepcíon, Chile.

Morgenstern Jr., A. and Moraes Jr., P., 2003, "Base Flow Investigation of a Recoverable Orbital Capsule," AIAA paper AIAA-2003-1252.

Morgenstern Jr., A., Fico Jr., N. G. C. R. and Valadão, H., 2007, "Evaluation of the Spallart-Almaras Turbulence Model in a Transonic Diffuser", Proceedings of the CMNE/CILAMCE 2007, Porto, 13-15 Junho.

Rogan. J.E. and Hurwicz, H., 1973, "High-temperature Thermal Protection Systems," *Handbook of Heat Transfer*, edited by Rohsenow, W.M. and Hartnett J.P., McGraw-Hill, New York.

Ruperti Jr., N.J., 1991, "Solution of a One-Dimensional Ablation Model", M.Sc. Dissertation, National Institute for Space Research – INPE, São José dos Campos, Brazil (in Portuguese).

Silva, D.V.F.M.R., 1976, "Estimative of Thermal Properties of Ablative Materials," M.Sc. Dissertation, Federal University of Rio de Janeiro - UFRJ, Rio de Janeiro, Brazil, 2001 (in Portuguese).

U.S. Standard Atmosphere.

Unverdi, S.O. and Tryggvason, G., 1992, "A Front-Tracking Method for Viscous, Incompressible, Multi-fluid Flows," *Journal of Computational Physics*, Vol. 100, pp. 25-37.

Zoby, E.V., Moss, J.N. and Sutton, K., 1981, "Approximate Convective Heat Equations Hypersonic Flows," *Journal of Spacecraft and Rockets*, Vol. 18, No. 1, pp. 64-70.